

tion of the calculated ratio ($g_{11\text{LaCl}_3}/g_{11\text{La}(\text{C}_2\text{H}_5\text{SO}_4)_3 \cdot 9\text{H}_2\text{O}}$) from the experimental ratio is 1.1%.) The values of the nuclear magnetic moments, 1.097 ± 0.11 and 0.682 ± 0.07 agree with the values of Halford⁶ (1.079 ± 0.06 , and 0.671 ± 0.04) and with those of Unsworth³⁸ (1.0644 ± 0.0040 and 0.6534 ± 0.0040).

4.3. Additional Comments

The measured ratios of the magnetic dipole moments of the two isotopes is essentially determined by the ratio of the two transition frequencies $k=0 \rightarrow k=0$ because of the small line width of these transitions (1 Mc/sec). This provides a simple method of determining the ratio of the magnetic dipole moments of two isotopes. (The ratio is independent of the salt in which the measure-

ment is made and independent of the temperature of the salt from 4° to 14°K for Nd³⁺.)

Further investigation of Nd³⁺ in $\text{La}(\text{C}_2\text{H}_5\text{SO}_4)_3 \cdot 9\text{H}_2\text{O}$ is required to elucidate the nature of the anomalous behavior at zero magnetic field. ENDOR studies at zero magnetic field and at high magnetic field should be undertaken.

ACKNOWLEDGMENTS

I wish to thank C. A. Hutchison, Jr., for many stimulating discussions, many helpful suggestions, and much encouragement during these experiments. I acknowledge the suggestion of M. Klein for the design of the microwave oscillator. I thank E. Bartal, C. E. Davoust, and W. Geiger for construction of some of the apparatus.

Longitudinal Plasma Oscillations near Electron Cyclotron Harmonics

S. J. BUCHSBAUM AND AKIRA HASEGAWA*

Bell Telephone Laboratories, Murray Hill, New Jersey

Received 23 August 1965)

A theory is developed for longitudinal plasma oscillations (normal modes) which are excited in a warm plasma column at microwave frequencies in the presence of a strong magnetic field. The oscillations manifest themselves as a set of absorption peaks near the harmonics of the electron cyclotron frequency. Good agreement is found between the observed positions of the peaks and a model calculation. The important property of the oscillations is that they are confined to a region near the axis of the plasma column, and are "quantized" by the shape of the electron density distribution.

I. INTRODUCTION

ACAREFULLY obtained microwave absorption spectrum of a plasma column in the presence of a longitudinal magnetic field exhibits considerable structure near the electron cyclotron harmonics (Fig. 1). The structure contains many lines (denoted a, b, c, d . . . in Fig. 1) at magnetic fields somewhat larger than the cyclotron harmonic fields $B = m\omega/en$, superimposed on a background absorption which is only a weak function of magnetic field. Here n is an integer and ω the microwave frequency. The structure is most prominent near the second harmonic, but it has been clearly discerned, albeit with diminishing amplitude, near the third, fourth and fifth harmonics. To observe such absorption either microwave cavities or waveguides can be used, but the modes must be such that the electric field of the wave is polarized at right angles to the static magnetic field, that is, the electromagnetic field must have, at least in part, the polarization of an extraordinary wave. It is well known¹ that such a wave, when it propagates

nearly at right angles in a cold plasma, possesses a (hybrid) resonance at $\omega^2 = \omega_p^2 + \omega_b^2$, where ω_p and ω_b are the electron plasma and cyclotron frequencies, respectively. Indeed, the background absorption in Fig. 1 results from the absorption caused by the hybrid resonance.²

The line spectrum was first observed in emission by Mitani, Kubo and Tanaka,³ and probably even earlier by Ishii.⁴ It has since been studied in absorption by us,⁵ by Crawford, Kino, and Weiss, by Harp,⁶ and by Schmitt, Meltz, and Freyheit.⁷ Schmitt reports as many as 30 lines near the second harmonic which he observed in an afterglow plasma using strip-line techniques

² S. J. Buchsbaum, *Bull. Am. Phys. Soc.* **7**, 151 (1962); G. Bekefi, J. D. Coccoli, E. B. Hooper, and S. J. Buchsbaum, *Phys. Rev. Letters* **9**, 6 (1962).

³ K. Mitani, H. Kubo, and S. Tanaka, *J. Phys. Soc. Japan* **19**, 211 (1964).

⁴ S. Ishii (private communication).

⁵ S. J. Buchsbaum and A. Hasegawa, *Phys. Rev. Letters* **12**, 685 (1964).

⁶ F. W. Crawford, G. S. Kino, and H. H. Weiss, *Phys. Rev. Letters* **13**, 229 (1964). R. S. Harp, *Appl. Phys. Letters* **6**, 51 (1965).

⁷ H. J. Schmitt, G. Meltz, and P. J. Freyheit, *Phys. Rev.* **139**, A1432 (1965).

* Present address: Faculty of Engineering Science, Osaka University, Toyonaka, Osaka-Fu, Japan.

¹ W. P. Allis, S. J. Buchsbaum, and A. Bers, *Waves in Anisotropic Plasmas* (MIT Press, Cambridge, Massachusetts, 1963), p. 30.

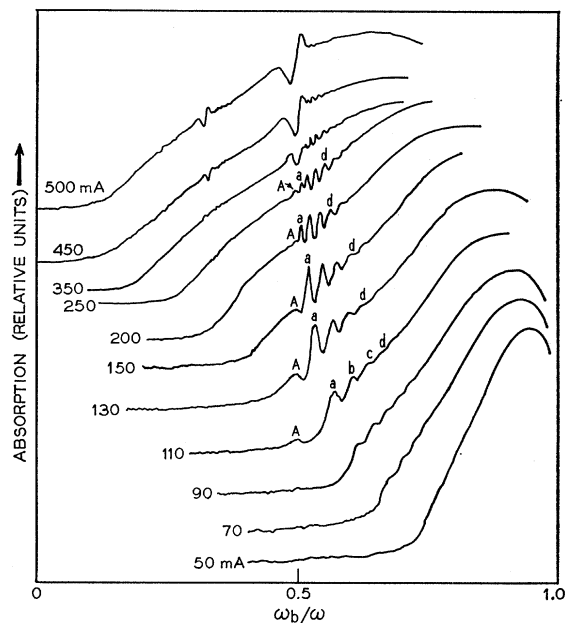


FIG. 1. Microwave absorption (in relative units) in a plasma column as a function of magnetic field with current I as a parameter. The curves for different I 's are displaced for display purposes. The plasma is the positive column (diameter = 0.8 cm, $p = 0.4$ Torr) of a hot-cathode discharge in helium.

similar to those employed in the study of Tonks-Dattner resonance.⁸

In a preliminary publication⁵ we put forth a model which accounted very well for the observed spectrum. We attributed the observed absorption lines to the excitation of longitudinal electron plasma oscillations within narrow pass-bands near each cyclotron harmonic. For a given frequency and plasma density, the width of the bands in magnetic field decreases as the harmonic number increases and is also a function of plasma frequency and electron temperature. Such pass-bands were discussed by Bernstein,⁹ for propagation of electrostatic plasma oscillations across a magnetic field in a uniform, infinite plasma. We showed, however, that as in the case of the so-called Tonks-Dattner⁸ resonance, radial density gradients in a plasma column of finite transverse dimensions play a profound role in determining the absorption or emission spectrum. There exists an important difference, however, in the role of density gradients in the two cases. In the absence of a magnetic field, the oscillations are essentially governed by the Bohm and Gross dispersion relation, $\omega^2 = \omega_p^2 + k^2 v^2$, where v is the electron thermal speed. Thus, they can be excited only at frequencies that are larger than the local plasma frequency ω_p . Consequently, in a plasma column of a finite radius, whose density decreases from the axis towards the walls, the Tonks-

Dattner oscillations are confined to a narrow annular region near the wall of the column,⁸ where the plasma frequency is below the oscillation frequency. As shown most impressively by Parker, Nickel, and Gould⁸ and by others,¹⁰ the actual frequency spectrum depends strongly on the properties of the sheath. In the presence of a magnetic field, Bernstein's uniform-plasma dispersion relation shows that within the above-mentioned pass bands the oscillations can be excited at frequencies that are lower than a certain critical frequency which is an increasing function of the local plasma frequency. This property of the oscillations confines them to the region near the axis of the plasma column and has the welcome consequence that the observed (and also calculated) spectra are relatively insensitive to conditions in the sheath.

In the preliminary publication⁵ we merely summarized the theory underlying the model and presented the results of a calculation for planar geometry. In the present paper we discuss the theory in greater detail and also extend the calculation to cylindrical (that is, experimental) geometries. We shall be forced to make a number of simplifying assumptions and yet we shall find excellent agreement between theory and experiment. Since this happy result does not necessarily justify all the assumptions, we shall attempt to provide the justification as we go along either on physical or mathematical grounds. The most important simplification that we shall make is that the observed spectrum is the result of purely longitudinal oscillations. That is, we shall use only Poisson's equation to describe the electromagnetic field, rather than the full set of Maxwell equations, and we shall disregard the fact that in the experiment nearly *transverse* electromagnetic waves are used to observe the phenomena under discussion here. It is clear that the electromagnetic and electrostatic waves must couple somewhere in the plasma. There is general agreement that the coupling occurs in that part of the plasma column where the conditions for the hybrid resonance $\omega^2 = \omega_b^2 + \omega_p^2(r)$ are satisfied. But the exact nature of the coupling remains obscure although it is the subject of considerable present study.¹¹ Thus we shall not be able to say anything about the strength of the observed spectrum relative to the background absorption. Only the positions of the lines will be accurately described.

In Sec. II we derive the differential equation for the electrostatic potential $\Phi(r, t)$ from linearized Boltzmann and Poisson equations. We then discuss the solution of this equation for planar and cylindrical geometries and compare the solution with experiment.

⁸ J. V. Parker, J. C. Nickel, and R. W. Gould, *Phys. Fluids* **7**, 1489 (1964). This paper contains extensive references to past work on Tonks-Dattner resonances.

⁹ I. B. Bernstein, *Phys. Rev.* **109**, 10 (1958).

¹⁰ A. Dattner, *Ericsson Tech.* **8**, 1 (1963); F. W. Crawford, *Phys. Letters* **5**, 244 (1963); A. M. Messiaen and P. E. Vandeplass, *Physica* **28**, 537 (1963); F. C. Hoh, *Phys. Rev.* **133**, A1016 (1964).

¹¹ T. H. Stix, *Bull. Am. Phys. Soc.* **10**, 230 (1965); J. M. Dawson and A. F. Kuckes, *ibid.* **10**, 231 (1965); T. H. Stix, *Phys. Rev. Letters* **15**, 878 (1965).

II. THEORY

Consider a plasma in the presence of a static uniform magnetic field B_0 oriented along the z axis of a Cartesian (or a cylindrical) coordinate system. The plasma is assumed to be uniform along z , but nonuniform at right angles to z . As mentioned in the Introduction, we consider the oscillations to be purely longitudinal so that the electric field \mathbf{E} associated with the oscillations is derivable from a scalar potential Φ ; $\mathbf{E} = -\nabla\Phi$. We assume that the unperturbed electron distribution function $f_0(\mathbf{r}, \mathbf{v})$ has the form

$$f_0(\mathbf{r}, \mathbf{v}) = g(x, y) f_0(\mathbf{v}), \quad (1)$$

where $0 \leq g(x, y) \leq 1$. This choice for $f_0(\mathbf{r}, \mathbf{v})$ is adequate whenever the electron density gradients are very much steeper than the temperature gradients. Ultimately, we shall take $f_0(\mathbf{v})$ to be a Maxwellian at a temperature T (measured in electron volts). We assume that the axial wavelength of the oscillations is infinite, that is, we set $\partial\Phi/\partial z = 0$. The assumption is justified only when $|\omega - n\omega_b| \gg k_z v$, so that cyclotron damping and other effects which result from finite axial wavelength are negligible.¹² Here k_z is the axial wavenumber and v the thermal speed. This condition is satisfied over most, but not all, of the range of a typical experiment. Indeed, the disappearance in Fig. 1 of the line spectrum as the plasma frequency increases, when the lines crowd closer together and are very near the magnetic field given by $2\omega_b = \omega$, may well be the result of cyclotron damping of the oscillations.

Our basic equations are then the linearized Boltzmann and Poisson equations,

$$j\omega f_1 + \mathbf{v} \cdot \nabla f_1 - \frac{e}{m} \left(\mathbf{E}_1 \cdot \frac{\partial f_0}{\partial \mathbf{v}} + \mathbf{E}_0 \cdot \frac{\partial f_1}{\partial \mathbf{v}} \right) - \frac{e}{m} (\mathbf{v} \times \mathbf{B}_0) \cdot \frac{\partial f_1}{\partial \mathbf{v}} = 0, \quad (2)$$

and

$$\nabla^2 \Phi = \frac{eN_0}{\epsilon_0} \int f_1 d^3v, \quad \mathbf{E} = -\nabla\Phi, \quad (3)$$

where

$$\nabla \equiv \hat{e}_x \partial/\partial x + \hat{e}_y \partial/\partial y.$$

In Eq. (2) we assumed a harmonic time dependence of all linearized quantities as $\exp(j\omega t)$ and have neglected collisions. They can be reintroduced phenomenologically by replacing $(j\omega)$ with $(\nu + j\omega)$, where ν is the electron collision frequency for momentum transfer. In the experiment, collisions are responsible for the observed absorption. The neglect of collisions is thus another reason why we shall be able to describe only the position, but not the strength, of the observed peaks.

We shall now make a more stringent assumption and

neglect in Eq. (2) the term involving the static electric field \mathbf{E}_0 . Since we consider a plasma with finite density gradients, \mathbf{E}_0 does not vanish. Indeed, a finite \mathbf{E}_0 is required if the distribution given by Eq. (1) is to be a solution of the zeroth-order Boltzmann equation. Yet we show in the Appendix that for the problem at hand the neglect of the term in question is justified provided $r_c |\nabla N|/N \ll 1$ where r_c is the electron cyclotron radius.¹³ The inequality is clearly satisfied near the axis of a plasma column, but may fail in the sheath where there are strong density gradients. However, as we mentioned earlier, we shall find that the oscillations are trapped in the region near the axis and are affected only weakly by what happens in the sheath. Thus, Eq. (2) reduces to

$$j\omega f_1 + \mathbf{v} \cdot \nabla f_1 - \frac{eB_0}{m} \left(v_y \frac{\partial f_1}{\partial v_x} - v_x \frac{\partial f_1}{\partial v_y} \right) = -\frac{e}{m} \left(\frac{\partial \Phi}{\partial x} \frac{\partial f_0}{\partial v_x} + \frac{\partial \Phi}{\partial y} \frac{\partial f_0}{\partial v_y} \right). \quad (4)$$

It has been shown by Hasegawa¹⁴ that Eq. (4) may be integrated formally by treating $\partial/\partial x$ and $\partial/\partial y$ as operators. The result is

$$f_1 = -\frac{1}{2B_0} \sum_{k=-\infty}^{\infty} \sum_{l=-\infty}^{\infty} \sum_{m=-\infty}^{\infty} \sum_{n=-\infty}^{\infty} \times I_l(b_x) I_m(b_x) J_k(b_y) J_n(b_y) (-1)^l e^{j(k+l+m+n)\Psi} \times \left[\left(\frac{e^{j\Psi}}{a+l+k+1} - \frac{e^{-j\Psi}}{a+l+k+1} \right) \frac{\partial \Phi}{\partial x} + j \left(\frac{e^{j\Psi}}{a+l+k+1} + \frac{e^{-j\Psi}}{a+l+k+1} \right) \frac{\partial \Phi}{\partial y} \right] \frac{\partial f_0}{\partial u}, \quad (5)$$

where

$$\Psi = \tan^{-1} v_x/v_y, \quad u^2 = v_x^2 + v_y^2,$$

$$a = -\omega/\omega_b, \quad b_x = -(u/\omega_b)\partial/\partial x, \quad b_y = j(u/\omega_b)\partial/\partial y,$$

and the J_n and I_n are Bessel functions and modified Bessel functions of the first kind. Note that $\partial/\partial x$ and $\partial/\partial y$ now appear as arguments of Bessel functions and have physical meaning only when the functions can be expanded as power series in b_x and b_y , which then operate on Φ . Since $|b| \simeq r_c/\lambda$, where r_c is the cyclotron radius and λ the "wavelength" of the oscillation, the power series expansion is valid only when $r_c/\lambda < 1$. We shall show on a *posteriori* basis that this is indeed so.

¹³ Very recent work [G. A. Pearson and S. J. Buchsbaum, Bull. Am. Phys. Soc. (to be published)] has shown that the neglect of the term $\mathbf{E}_0 \cdot \partial f_1/\partial \mathbf{v}$ leads to errors in eigenfrequencies of the order $(\lambda \nabla N/N)^2$, where λ is the wavelength of the oscillations [Eq. (18)]. Such errors are indeed small under most experimental conditions. However, the neglect of \mathbf{E}_0 may lead to large errors in the eigenfunctions.

¹⁴ A. Hasegawa, Phys. Fluids 8, 761 (1965).

¹² T. H. Stix, *The Theory of Plasma Waves* (McGraw-Hill Book Company, Inc., New York, 1962), p. 159.

Since our aim is to solve Eqs. (3) and (4) for a bounded system (a plasma column of finite radius, or a plasma slab), a discussion of boundary conditions is in order. The conditions on the potential Φ are the ordinary boundary conditions of electrostatics, but what are the boundary conditions on the distribution function $f(\mathbf{r})$? This is a difficult problem whose solution is known only for very simple geometries.¹⁵ We shirk it here and replace the boundary condition on f by the macroscopic condition that the normal component of the conduction current vanish at the boundary of the plasma. This is not too drastic an approximation partly because the oscillations are trapped near the axis of the column and only "tunnel" out to the walls, and partly because of the neglect of \mathbf{E}_0 , Eq. (5) is incomplete near the walls.

The distribution function f_1 is now substituted in Eq. (3) and the integration over the velocity space performed. Integration over Ψ reduced the number of infinite sums to three, and the expansion of Bessel functions is now a straightforward but tedious task. As is well known from the solution of similar problems in uniform plasmas, to obtain the dispersion equation adequate for phenomena up to the second harmonic (that is, for $\omega_b/\omega > \frac{1}{2}$) it is sufficient to retain in the expansion only terms linear in the temperature, up to third-harmonic terms quadratic in temperature, and so on. An examination of the power series expansion of Bessel functions reveals that only the terms for which

$$|l| + |m| + |n| + |l+m-n| \leq 3$$

are at most linear in T . Retaining only such terms yields the following differential equation for Φ :

$$\nabla^2 \Phi = (\mathcal{E}_1 + \lambda_1^2 \nabla^2) \{ \nabla \cdot (g \nabla \Phi) \}, \\ + j(\mathcal{E}_2 + \lambda_2^2 \nabla^2) \left\{ \frac{\partial}{\partial y} \left(g \frac{\partial \Phi}{\partial x} \right) - \frac{\partial}{\partial x} \left(g \frac{\partial \Phi}{\partial y} \right) \right\}, \quad (6)$$

where

$$\mathcal{E}_1 = \omega_{p0}^2 / (\omega^2 - \omega_b^2), \quad \mathcal{E}_2 = (\omega_b/\omega) \mathcal{E}_1, \\ \lambda_1^2 = \frac{3\omega_{p0}^2 (eT/m)}{(4\omega_b^2 - \omega^2)(\omega^2 - \omega_b^2)} = \frac{3\omega_{p0}^4 \lambda_D^2}{(4\omega_b^2 - \omega^2)(\omega^2 - \omega_b^2)}, \\ \lambda_2^2 = 2(\omega_b/\omega) \lambda_1^2. \quad (7)$$

Here, $\omega_{p0}^2 = N_0 e^2 / m \epsilon_0$, N_0 being the electron density on the axis, that is, where $g(x, y) = 1$; $\lambda_D^2 = kT / m \omega_{p0}^2$ is the Debye length squared on the axis.

Note that for $T=0$, Eq. (6) properly reduces to

$$\nabla \cdot (\boldsymbol{\epsilon} \cdot \nabla \Phi) = 0, \quad (8)$$

where

$$\boldsymbol{\epsilon} \equiv \begin{vmatrix} 1 - \mathcal{E}_1 g & j \mathcal{E}_2 g & 0 \\ -j \mathcal{E}_2 g & 1 - \mathcal{E}_1 g & 0 \\ 0 & 0 & 1 - (\omega_{p0}^2 / \omega^2) g \end{vmatrix} \quad (9)$$

is the "cold-plasma" dielectric tensor.

Equation (6) is a fourth-order differential equation. For a uniform plasma, that is, when $g(x, y) = \text{const}$, it reduces to

$$\nabla^2 (\nabla^2 + \kappa^2) \Phi = 0 \quad (10)$$

which separates into

$$\nabla^2 \Phi = 0, \quad (11a)$$

$$(\nabla^2 + \kappa^2) \Phi = 0, \quad (11b)$$

where

$$\kappa^2 = (\mathcal{E}_1 - 1) / \lambda_1^2.$$

As discussed by Parker, Nickel, and Gould,⁸ Eq. (11a) gives the charge-free solution, that is, it gives transverse waves of infinite wavelength in the quasistatic approximation, while Eq. (11b) describes the longitudinal (plasma) waves. In a uniform plasma they are uncoupled as the separation indicates. In a nonuniform plasma the longitudinal and transverse waves are coupled by the density gradients, and the coupling is strong because the scale of the density gradients is smaller than the "infinite" wavelength of the transverse waves. In reality, the wavelength of the transverse waves is finite when they are described by the full set of Maxwell equations, so that the nature of the coupling will be different, especially near the hybrid resonance, $\omega^2 = \omega_p^2(r) + \omega_b^2$, where the wavelength of the transverse waves can become very short. Unfortunately, as mentioned in the Introduction, the exact nature of the true coupling remains to be worked out.

The second term on the right-hand side of Eq. (6) contains terms of the form $(\partial g / \partial x)(\partial \Phi / \partial y)$ and $(\partial g / \partial y)(\partial \Phi / \partial x)$. These are different from zero only for "two-dimensional" oscillations, that is, oscillations whose electric fields have components at right angles as well as parallel to density gradients. Such is the case when the oscillations are excited in a waveguide, for example. We have not yet examined this more general case in sufficient detail to discuss it in the present paper. Instead, we limit ourselves here to the "one-dimensional" case in which the electric field components exist only parallel to the density gradients. Such is the case when the oscillations are excited by means of an axially symmetric mode of cylindrical cavity (the TE_{011} -mode, for example). Such a mode was used to obtain the data in Fig. 1.

We take, therefore, g to be only a function of one coordinate, say x , and set $\partial / \partial y = 0$ in Eq. (6). This equation then reduces to

$$\frac{d}{dx} \left[\frac{d^2}{dx^2} \left(g \frac{d\Phi}{dx} \right) + \frac{1}{\lambda_1^2} \left(\mathcal{E}_1 - \frac{1}{g} \right) \left(g \frac{d\Phi}{dx} \right) \right] = 0. \quad (12)$$

We shall discuss Eq. (12) for both planar and cylindrical geometries.

A. Planar Geometry

To avoid the difficulties which arise from matching boundary conditions and to gain a clearer insight into

¹⁵ G. H. Reuter and E. H. Sondheimer, Proc. Roy. Soc. (London) **A195**, 336 (1949) P. M. Platzman and S. J. Buchsbaum, Phys. Rev. **132**, 2 (1963).

the nature of the oscillations, we consider first an "infinite slab," that is, we assume that $g(x)$ does not vanish except at infinity. We take for $g(x)$ the function

$$g(x) = (1 + \gamma x^2/d^2)^{-1}, \quad (13)$$

This form is particularly convenient because it allows Eq. (12) to be solved exactly. Integrating Eq. (12) once and defining a weighted electric field $\mathcal{R} \equiv g d\Phi/dx$ yields

$$d^2\mathcal{R}/dx^2 + (1/\lambda_1^2)(\mathcal{E}_1 - 1 - \gamma x^2/d^2)\mathcal{R} = 0, \quad (14)$$

Equation (14) has the form of a Schrödinger equation for a simple harmonic oscillator. Its solutions are well known and are given in terms of the parabolic cylinder functions,¹⁶

$$\mathcal{R} = D_\nu(x/\lambda) \pm D_{-\nu}(x/\lambda), \quad (15)$$

where

$$\lambda = [\lambda_1 d / 2\gamma^{1/2}]^{1/2} \\ = [3\omega_{p0}^4 d^2 \lambda_D^2 / 4\gamma(\omega^2 - \omega_b^2)(4\omega_b^2 - \omega^2)]^{1/4}, \quad (16)$$

and

$$\nu = \frac{1}{2} \left\{ [(\mathcal{E}_1 - 1)d / \gamma^{1/2} \lambda_1] - 1 \right\} \\ = \frac{1}{2} \left[\left\{ \frac{(4\omega_b^2 - \omega^2)d^2 / \lambda_D^2}{3\gamma\omega_{p0}^4(\omega^2 - \omega_b^2)} \right\}^{1/2} (\omega_b^2 + \omega_{p0}^2 - \omega^2) - 1 \right]. \quad (17)$$

The function $D_\nu(x/\lambda)$ is an oscillatory function for small x , that is, where the "kinetic" energy $(\mathcal{E}_1 - 1)/\lambda_1^2$ exceeds the "potential" energy. At large x it exhibits a tunneling-like behavior. It has $\nu + 1$ zeros which are spaced by approximately λ . Thus the quantity λ can be considered to be the "wavelength" of the oscillation. Since, under experimental conditions $d \gg \lambda_D$, we find that $d > \lambda > \lambda_D$. We can now check whether or not the expansion parameter (r_c/λ) is smaller than unity. We find from Eq. (15)

$$r_c/\lambda = (\lambda_D/d)^{1/2} [(4\gamma/3)(\omega^2/\omega_b^2 - 1)(4 - \omega^2/\omega_b^2)]^{1/4}. \quad (18)$$

The square bracket in Eq. (17) is of order unity, except when $\omega \approx 2\omega_b$, so that we have to rely on λ_D being very much smaller than the scale size of the density gradient d , for (r_c/λ) to be smaller than unity. For our experimental conditions $\lambda_D \approx 4 \times 10^{-3}$ cm and $d \approx 0.5$ cm, so that $(r_c/\lambda) \approx \frac{1}{10}$.

The function D_ν is square integrable only when ν is an integer (or zero) and this condition leads to the dispersion relation of the oscillation. Thus $\nu = l$ where $l = 0, 1, 2, 3, \dots$ yields the following dispersion relation¹⁷ for the oscillations:

$$(\mathcal{E}_1 - 1)d / \gamma^{1/2} \lambda_1 = (2l + 1), \quad (19a)$$

or

$$(4\omega_b^2 - \omega^2)(\omega_b^2 + \omega_{p0}^2 - \omega^2) \left(\frac{\omega_{p0}^2}{\omega^2 - \omega_b^2} - 1 \right) \\ = (2l + 1)^2 3\gamma\omega_{p0}^4 \lambda_D^2 / d^2. \quad (19b)$$

It is worthwhile to point out that precisely the same relation would result if the WKB method were used to quantize the "phase" in Eq. (14) between the two turning points, $x_\pm = \pm [d^2(\mathcal{E}_1 - 1)/\gamma]^{1/2}$. This is not surprising since the WKB solution is known to be exact for the simple harmonic oscillator.

Using Eq. (19) in (16) the "wavelength" λ becomes

$$\lambda = d \left\{ \frac{[\omega_{p0}^2 / (\omega^2 - \omega_b^2)] - 1}{2\gamma(2l + 1)} \right\}^{1/2} \quad (20)$$

so that, indeed, $\lambda < d$.

It is instructive to compare Eq. (19) with the corresponding dispersion relation for a uniform plasma. Expanding Bernstein's dispersion relation

$$1 = \left(\frac{\omega_{p0}^2}{\omega_b^2} \right) \sum_{n=1}^{\infty} \frac{2n^2 \exp(-\mu) I_n(\mu)}{\mu [(\omega^2/\omega_b^2) - n^2]} \quad (21)$$

in power of temperature and retaining only terms linear in T yields

$$(4\omega_b^2 - \omega^2)(\omega_b^2 + \omega_{p0}^2 - \omega^2) = 3\omega_{p0}^4 \kappa^2 \lambda_D^2, \quad (22)$$

where $\mu = \kappa r_c$ and $\kappa = 2\pi/\lambda$, with λ the wavelength of the oscillation. The essential difference between Eqs. (22) and (19b) is that the term $(\omega_b^2 + \omega_{p0}^2 - \omega^2)$ appears squared in Eq. (19b). The difference is partly removed if the "proper" λ is used in Eq. (22), for example, that given by Eq. (20).

Equation (19b) is plotted as the dashed curves in Fig. 2 for $\gamma T/d^2 = 3$ eV/cm². The subscripts + and -

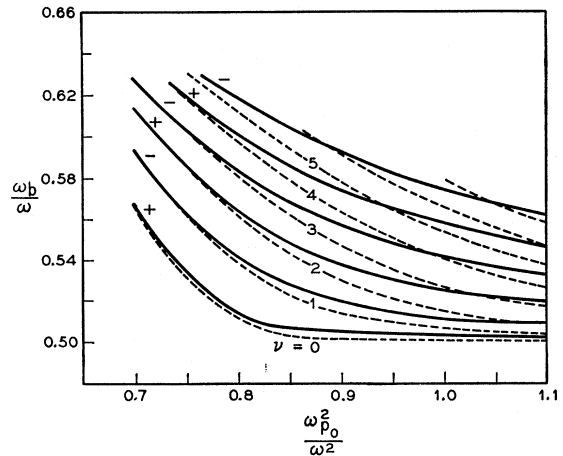


FIG. 2. Calculated resonant frequencies of the odd (-) and (+) solutions in a plasma slab. The solid lines are the solution of Eq. (19b) for an infinite slab; the dashed lines are for a finite slab and are obtained from Eq. (23).

¹⁶ E. T. Whittaker and G. N. Watson, *Modern Analysis* (Cambridge University Press, New York, 1962), p. 337.

¹⁷ We use the term "dispersion relation" even though the frequency does not depend explicitly on wave number.

refer to even and odd solutions about $x=0$. It can be seen from Eq. (19b), that the ratio (ω_b/ω) is a function of two parameters, (ω_{p0}^2/ω^2) and $(\gamma T/d^2)$. The first of these can usually be measured experimentally from the onset of the "cold-plasma" background absorption, or by other means. The second parameter is not generally amenable to precise measurement and is best fitted.

The solid curves in Fig. 2 are for a finite slab of thickness $2d$, that is, we took $g(x)$ to have the form given by Eq. (13) only for $|x| \leq d$ and to be zero for $|x| > d$. The proper boundary condition for both the current and potential is

$$D_y(d/\lambda) \pm D_{-y}(d/\lambda) = 0 \quad (23)$$

which constitutes the dispersion relation. As can be seen from Fig. 2, the solution for finite slab is nearly identical to that for the infinite plasma when $(\omega_{p0}^2 + \omega_b^2)$ is near ω^2 . Then the turning points x_t are near the axis of the slab and are far from the walls at $\pm d$, so that the boundary conditions at the walls do not matter. As ω_{p0}^2/ω^2 is increased, however, the turning points move closer to the walls of the slab, and the influence of the boundary condition begins to be felt.

B. Cylindrical Geometry

In cylindrical coordinates Eq. (14) is

$$\frac{d^2 \mathcal{R}}{dr^2} + \frac{1}{r} \frac{d\mathcal{R}}{dr} + \frac{1}{\lambda_1^2} \left(\mathcal{E}_1 - 1 - \gamma \frac{r^2}{d^2} - \frac{\lambda_1^2}{r^2} \right) \mathcal{R} = 0, \quad (24)$$

where $\mathcal{R} = g(r) d\Phi/dr$ and \mathcal{E}_1 and λ_1 are defined in Eq. (7). Again we took $g(r) = (1 + \gamma r^2/d^2)^{-1}$ to facilitate solving Eq. (24). Equation (24) can be put in the form of a Whittaker equation.¹⁸ If we set $r^2 = y$ and $\mathcal{R} = G/\sqrt{y}$ we obtain

$$d^2 G/dy^2 + (1/4\lambda_1^2) [(\mathcal{E}_1 - 1)/y - \gamma/d^2] G = 0. \quad (25)$$

Since the Whittaker function $W_{k,m}$ is a solution of¹⁸

$$\left(\frac{d^2}{dz^2} - \frac{1}{4} + \frac{k}{z} + \frac{\frac{1}{4} - m^2}{z^2} \right) W_{k,m} = 0 \quad (26)$$

the solution of Eq. (24) is

$$\mathcal{R} \approx r^{-1} W_{\mu, \pm \frac{1}{2}}(r^2/2\lambda^2), \quad (27)$$

where $\mu = (\mathcal{E}_1 - 1)d/4\gamma^{1/2}\lambda_1$, and λ is as given in Eq. (16). Proceeding as for the planar geometry it can be shown that the dispersion relation for an "infinite" cylinder [i.e., when we allow $g(r)$ to be $(1 + \gamma r^2/d^2)^{-1}$ for all r] is precisely that for the "infinite" plane slab except that the term $(2l+1)$ in Eq. (19) is to be replaced by $2(l+1)$. For a finite cylinder, we again take $g(r) = [1 + \gamma r^2/d^2]^{-1}$ for $r \leq d$ and $g(r) = 0$ for $r > d$. To obtain the dispersion relation it is simpler to integrate Eq. (24) on the computer and seek on it the family of

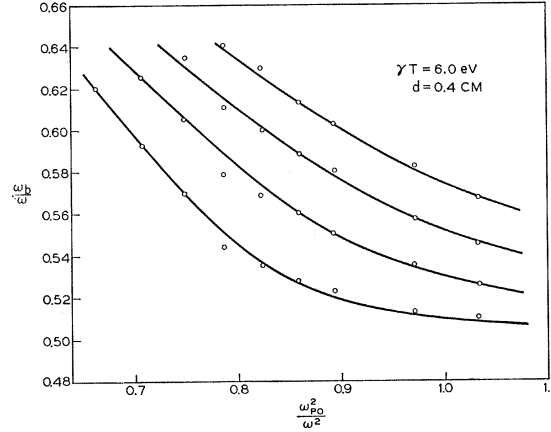


FIG. 3. Resonant frequencies in a cylindrical plasma. The solid curves are from Eq. (24). The points are experimental and correspond to absorption peaks in Fig. 1.

values of ω_b/ω and of ω_{p0}^2/ω^2 (for a given γT and d) for which $\mathcal{R}(d)$ vanishes, than it is to evaluate the Whittaker functions subject to the boundary conditions. In Fig. 3 are shown the results of such computation where we attempted to fit the experimental results of Fig. 1. The solid curves in Fig. 3 are calculated for $\gamma T = 6$ eV and $d = 0.4$ cm and the points are experimental.⁵ Here γT was varied until the vertical spacing between the two lowest solid curves was equal to the experimentally observed spacing at some value of ω_{p0}^2/ω^2 . That is, two and only two of the experimental points are fitted. The rest fall where they may.

As γT is increased, the "infinite" column dispersion relation predicts, and computations for a finite cylinder bear out the prediction, that the separation between the resonance peaks should increase approximately as the square root of the temperature. It was not possible to measure the electron temperature directly in our experiment, but on decreasing the working pressure in the discharge (which should lead to a high T) the separation between the resonance peaks was indeed observed to increase.

III. CONCLUSIONS

We presented a theoretical model which in spite of the many approximations and assumptions appears to account very well for the observed structure in microwave absorption near the second cyclotron harmonic. The theory can be extended to the third and higher harmonics by retaining successively higher order terms in temperature in the infinite series expansion of Eq. (5). This was done by Azevedo¹⁹ and will be published elsewhere.

ACKNOWLEDGMENTS

We thank Dr. S. Gruber and Dr. G. A. Pearson for comments on the manuscript.

¹⁸ E. T. Whittaker and G. N. Watson, *Modern Analysis* (Cambridge University Press, New York, 1962), p. 347.

¹⁹ J. Azevedo (private communication).

APPENDIX

In the linearized Boltzmann equation

$$\frac{\partial f_1}{\partial t} + \mathbf{v} \cdot \nabla f_1 + \frac{e}{m} \left(\mathbf{E}_1 \cdot \frac{\partial f_0}{\partial \mathbf{v}} + \mathbf{E}_0 \cdot \frac{\partial f_1}{\partial \mathbf{v}} \right) + \frac{e}{m} (\mathbf{v} \times \mathbf{B}_0) \cdot \frac{\partial f_1}{\partial \mathbf{v}} = 0,$$

we wish to neglect the term containing the static field \mathbf{E}_0 . In a positive column of an active discharge, \mathbf{E}_0 has both axial and radial components. The axial component is required to maintain the plasma, but we ignore it in Eq. (2) because it does not play a role in our problem. The component of interest is the radial electric field E_{r0} which accompanies the steady-state diffusion to the walls of the column. For our purposes it is sufficient to assume that the diffusion to the insulating walls is ambipolar. Then E_{r0} is given by²⁰

$$E_{r0} = \frac{(1 + \mu_-^2 B^2) \nabla(D_+ N) - (1 + \mu_+^2 B^2) \nabla(D_- N)}{(1 + \mu_+ \mu_- B^2)(\mu_+ + \mu_-) N}, \quad (\text{A1})$$

where μ_{\pm} and D_{\pm} are the ion (or electron) mobilities and

²⁰ D. R. Whitehouse and H. B. Wollman, *Phys. Fluids* **6**, 1470 (1963).

diffusion coefficients, respectively. Under conditions of the present experiment, $\mu_+ B \ll 1$, $\mu_- B \gg 1$ and $\mu_+ \mu_- B^2 \gtrsim 1$. Then (A1) reduces to

$$E_{r0} \sim \left(T_+ - \frac{T_-}{1 + \mu_+ \mu_- B^2} \right) \nabla N / N, \quad (\text{A2})$$

where T_- and T_+ are the electron and ion temperatures (in eV), respectively. In deriving (A2) we used the Einstein relation, $D_{\pm}/\mu_{\pm} = T_{\pm}$. Consequently, in order that the term $\mathbf{E}_0 \cdot (\partial f_1 / \partial \mathbf{v})$ be negligible compared to, say, $(\mathbf{v} \times \mathbf{B}_0) \cdot (\partial f_1 / \partial \mathbf{v})$, we must have

$$\left| \frac{T_+}{T_-} - \frac{1}{1 + \mu_+ \mu_- B^2} \right| \frac{r_c |\nabla N|}{N} \ll 1, \quad (\text{A3})$$

where r_c is the electron Larmor radius. In the present experiments, the neutral gas pressure is relatively high (0.1–0.5 Torr) so that $\mu_+ \mu_- B^2 \simeq 1$, and the inequality (A3) becomes

$$r_c |\nabla N| / N \ll 1. \quad (\text{A4})$$

The lower the pressure of the neutral gas, the easier it becomes to satisfy the inequality (A3).

Fe⁵⁷ Mössbauer Effect in Nickel Oxide*

V. G. BHIDE AND G. K. SHENOY

Physics Department, Institute of Science, Bombay, India

(Received 18 October 1965)

The Fe⁵⁷ Mössbauer effect in antiferromagnetic NiO, used as a source, has been studied over a wide range of temperatures below as well as above its Néel temperature (523°K). The aftereffects of decay produce only ferrous and ferric states, which have been identified by their characteristic hyperfine fields and isomer shifts. These observations are similar to those reported on CoO. The temperature dependence of the hyperfine field at the nuclei of Fe²⁺ and Fe³⁺ ions, although almost identical, deviates from the sublattice magnetization of NiO as well as from the Brillouin function for the Ni²⁺ state ($S=1$). The spectrum at liquid-nitrogen temperature indicated the presence of an electric field gradient at the ferrous nucleus. The intensity of the ferrous peak is highly temperature-dependent, decreasing with an increase in temperature finally vanishing above about 466°K. This dependence has been qualitatively explained in terms of the electron-capture mechanism. It has been concluded that the temperature dependence of the capture cross section of the ferric ion is mainly responsible for the observed behavior.

I. INTRODUCTION

NICKEL OXIDE is an antiferromagnetic substance¹ with a Néel temperature of 523°K, and is one of the most extensively studied monoxides of the iron group. It has a crystal structure characterized by an fcc lattice of the positive ions. Below the Néel temperature, the lattice contracts along one of its body diagonals, the corner angle becoming $\pi/2 \pm \Delta$. The cube

edges contract by an amount $\delta a/a$. The new geometry is rhombohedral.² The interaction of individual magnetic ions with the crystalline electric field from the distorted oxygen octahedra quenches the orbital angular momentum of the Ni²⁺ ions. Hence, in this substance the anisotropy energy responsible for the observed magnetic ordering (of the second kind) is mainly dipolar in origin.^{3,4} Further, the exchange forces con-

* Work done under the auspices of the National Bureau of Standards, Washington, D. C.

¹ T. Nagamiya, K. Yoshida, and R. Kubo, *Advan. Phys.* **4**, 6 (1955).

² Y. Shimomura and Z. Nisiyama, *Mem. Inst. Sci. Ind. Res., Osaka Univ.* **6**, 30 (1948).

³ J. Kaplan, *J. Chem. Phys.* **22**, 1709 (1954).

⁴ F. Keffer and W. O'Sullivan, *Phys. Rev.* **108**, 637 (1957).